Quantization and Colored Noises Error Modeling for Inertial Sensors for GPS/INS Integration

Songlai Han and Jinling Wang

***Abstract*—In this paper, modeling approaches for quantization and colored noises have been proposed. To accommodate the quantization noise, a modified inertial navigation system (INS) error dynamics is developed in this paper, and the quantization noise is incorporated into the modified INS error dynamics as augmenting driving noise. The three kinds of colored noises are modeled by using an equivalent differential equation driven by a unit white noise, and a technique is developed in this paper to augment the Kalman Filter of GPS/INS integration using this equivalent differential equation. Experimental test results show that the proposed stochastic error modeling approaches for quantization and colored noises significantly improves the accuracies of the estimated inertial drifts and the navigation solutions.**

***Index Terms*—Error modeling, GPS/INS, integration, inertial sensor, Kalman Filter.**

I. Introduction

INERTIAL NAVIGATION SYSTEM (INS) is a time-dependent system, and its performance will degrade with time [1]. This performance degradation is mainly caused by inertial sensors' errors, which can be classified into deterministic errors and stochastic errors according to their sources. So calibrations to the inertial sensors are necessary to improve the INS performances. The calibration for the deterministic errors can be achieved offline by using rate table before applications [2], while it is not in the scope of this paper. The compensation for the stochastic errors should be done online with the aiding of external facilities. Before the calibration can be carried out, the stochastic errors in inertial sensors should be well modeled. This paper will focus on the stochastic error modeling of the inertial sensors and its applications in Global Positioning System (GPS)/INS integration.

Various approaches have been studied to model the stochastic errors in an inertial sensor. In [3] and [4], the stochastic errors in gyro were assumed to be nonstationary and were described by using an ARMA model. In [5] and [6], the stochastic errors in inertial sensors were modeled as a simplified ARMA model, namely, autoregressive (AR) model. In [7]–[10], the stochastic errors in inertial sensors were assumed to be a stationary Gaussian–Markov process. In [11]–[14], the stochastic errors in inertial sensors were assumed to be the hybrid of a random walk process and a white noise process. References [15] and [16] pointed out that the ARMA model, or the AR model, is model-sensitive and is not suited to handling odd power processes, higher-order processes, or wide dynamic ranges. Reference [17] pointed that the drifts of the inertial sensors are nonstationary, so the Gaussian–Markov process, as a stationary process, can only act as an approximation for the real stochastic process. At the same time, the order, the coefficients, and the time constant of a Gaussian–Markov process are very difficult to determine to approximate a specific stochastic process. So, in this paper, considering the random walk is a crucial stochastic error in inertial sensors and its easy implementation, the hybrid of the random walk and the white noise is named as "conventional approach" and is used to compare with the proposed approach.

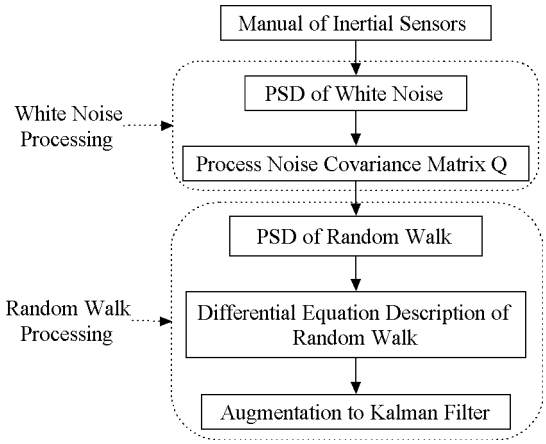

Fig. 1. Stochastic error modeling and processing flowchart under the assumption that the stochastic errors are the hybrid of white noise and random walk.

The power spectral density functions (PSDs) of the white noise and random walk can generally be obtained from the user manual or data sheet of the inertial sensors. The white noise was directly incorporated into the INS error dynamics as the driving noise, and its PSD was used to obtain the process noises covariance matrix, Q, which is needed in the Kalman Filter of GPS/INS integration. The random walk was described by a differential equation with a white noise as the driving function. The differential equation was derived from the PSD of the random walk, and was used to augment the Kalman Filter of GPS/INS integration. The procedure of this conventional approach is shown in Fig. 1.

Manuscript received January 11, 2010; revised April 20, 2010, July 19, 2010, and September 21, 2010; accepted November 10, 2010. Date of publication November 18, 2010; date of current version April 20, 2011. This work was supported in part by the Chinese Scholarship Council. The associate editor coordinating the review of this paper and approving it for publication was Prof. Okyay Kaynak.

S. Han is with the College of Opto-Electric Science and Engineering, National University of Defense Technology, Changsha 410073, Hunan, China, and also with the School of Surveying and Spatial Information System, University of New South Wales, NSW 2052, Australia (e-mail: songlai.han@student.unsw.edu.au).

J. Wang is with the School of Surveying and Spatial Information System, University of New South Wales, NSW 2052, Australia (e-mail: Jinling.Wang@unsw.edu.au).

Color versions of one or more of the figures in this paper are available online at http://ieeexplore.ieee.org.

Digital Object Identifier 10.1109/JSEN.2010.2093878

However, this conventional approach is based on the assumption that the stochastic errors in an inertial sensor are the hybrid of white noise and random walk. Actually, the true components of the stochastic errors in an inertial sensor may be much more complicated. For most applications, this assumption is an approximation which simplifies the modeling problem at the price of sacrificing the performances.

The advent of the Allan Variance analysis technique has changed this situation. The Allan Variance analysis technique was initially developed by David Allan of the National Bureau of Standards to quantify the error statistics for a Caesium beam frequency standard [20]. The technique was then expanded to identify and quantify the error characteristics of any precise instruments, and was accepted as an IEEE standard for gyro specifications [21]. Now, it has been accepted as a standard to obtain the noise parameters of the inertial sensors [22], [23].

Based on the stochastic error identification technique by using the Allan Variance analysis [11], [21], [23]–[26], this paper proposes the stochastic modeling approaches for the quantization and colored noises, which belong to a four-stage scheme for the stochastic error modeling and processing of the inertial sensors. The flowchart of this scheme is shown in Fig. 2.

In the first stage, Allan Variance analysis is used to identify the stochastic errors existing in inertial sensors, and the PSDs of the stochastic errors are determined. Then, the white noise is dealt with by using the same method as in the conventional approach shown in Fig. 1. In the third stage, the quantization noise is processed. The quantization noise is a special noise. According to the power spectral density function (PSD) of quantization noise [21], the differential equation description of quantization noise can be derived as follows:

$$d_{\mathrm{qn}}(t) = Q\sqrt{T}\dot{u}(t) \tag{1}$$

where $u(t)$ is a unit white noise. From (1), it can be noted that the derivative order of the driving white noise is higher than that of the quantization noise. From the point of view of the stochastic processes theory, $d_{\mathrm{qn}}(t)$ defined by (1) has infinite variance [27], so the system represented by (1) cannot be implemented physically. This paper proposes a new procedure to deal with the quantization noise, as shown in Fig. 2. In this proposed procedure, INS error dynamics is modified to incorporate the quantization noise into the dynamics as the driving noise, and the process noise covariance matrix, Q, obtained in the second stage by using the white noise is augmented by using the quantization noise. The detailed discussion about quantization noise is postponed to Section II. In the last stage, the colored noises are processed. Any noises with finite frequency bandwidths can be called colored noises. Herein, in the field of stochastic error modeling of inertial sensors, the colored noises refer to bias instability, random walk and ramp noise. In this paper, an equivalent differential equation representation for these three kinds of colored noises was developed, and a technique is developed by using the equivalent differential equation representation to augment the Kalman Filter of GPS/INS integration.

In this four-stage scheme, the components of the stochastic errors in an inertial sensor are identified by Allan Variance analysis, and some special techniques are developed in this paper to model these identified stochastic errors and to augment the Kalman Filter for GPS/INS integration, while in the conventional approach the components of the stochastic errors were simply assumed to be the hybrid of white noise and random walk. Experimental test results show that this four-stage scheme, shown in Fig. 2, for the stochastic error modeling of inertial sensors has a better performance than the conventional approach shown in Fig. 1.

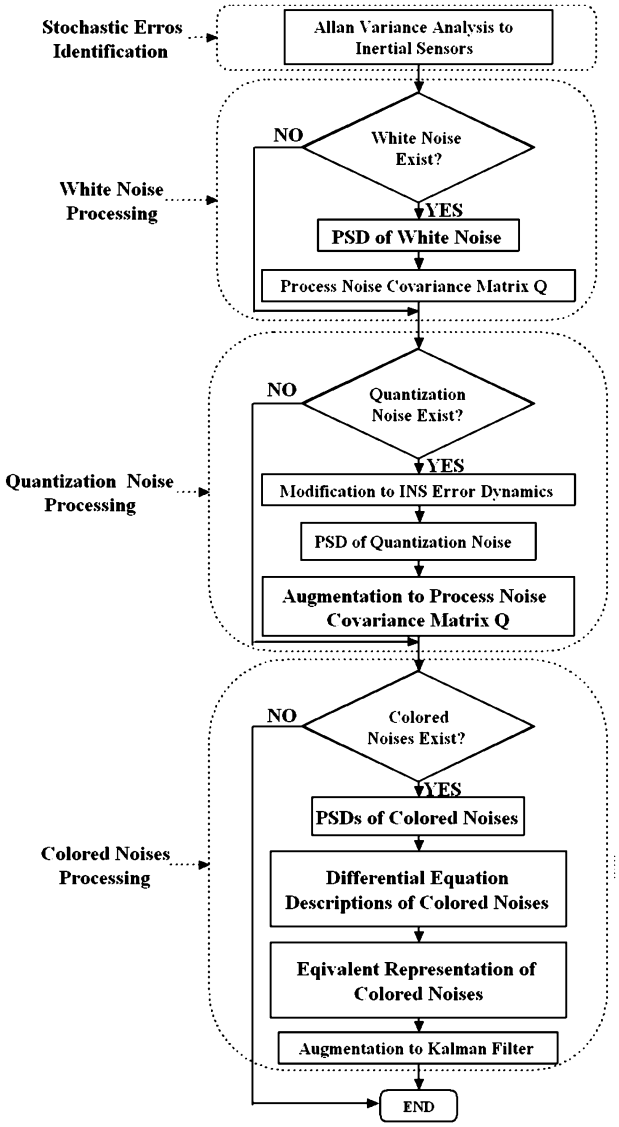

Fig. 2. Stochastic error modeling and processing flowchart based on stochastic error identification using the Allan Variance analysis technique and the equivalent representation of multiple stochastic errors.

The subject matter of this paper is presented as follows. Section II develops the modified INS error dynamics to model the quantization noise for GPS/INS integration. Section III derives the equivalent representation of multiple colored noises, which is then used to augment the Kalman Filter for GPS/INS integration. Section IV is devoted to the experimental tests, and Section V gives the concluding remarks.

II. Modeling and Processing of the Quantization Noise

The problems of quantization noise discussed in Section I arise from the sampling mechanism of the inertial sensors. For a gyro, not the angular rate but the delta angle is sampled, quantized and output, and not the angular rate quantization noise but

the delta angle quantization noise is produced during this procedure. According to [28], the delta angle quantization noise is white noise, and the angular rate quantization noise is equal to the derivative of the delta angle quantization noise. A similar conclusion can also be drawn for accelerometers. Based on the above analysis, [28] and [29] proposed an approach to incorporate the delta angle quantization noise and delta velocity quantization noise into the INS error dynamics. Because the delta angle quantization noise and delta velocity quantization noise are white noises, they can directly act as the driving noise and no further modeling work is necessary. However, [28] only considered the situation where the INS error dynamics were realized in the inertial frame. Although, in [29], some other possibilities about the frame of the INS error dynamics were discussed, the psi-angle error equations in the local level geographic frame were not included. Because our integration algorithm is implemented by using the psi-angle error equations, the counterpart results for the psi-angle error equations in the local geographic frame are developed herein for the first time.

The psi-angle error equations of INS in local the level geographic frame are [30]

$$\delta\dot{n} = \delta v - \omega_{\text{en}} \times \delta n \tag{2}$$

$$\delta\dot{v} = -\left(\omega_{\text{in}}^n + \omega_{\text{ie}}^n\right) \times \delta v - \psi \times f^b + \delta g^n + C_b^n \nabla^b \tag{3}$$

$$\dot{\psi} = -\omega_{\text{in}}^n \times \psi + C_b^n \varepsilon^b \tag{4}$$

where ∇^b and ε^b are the stochastic error vectors of the accelerometers and the gyros used, respectively, and they can be expressed as follows:

$$\nabla^b = \delta f_{\text{white}}^b + \delta f_q^b + \delta f_{\text{colored}}^b \tag{5}$$

$$\varepsilon^b = \delta\omega_{\text{white}}^b + \delta\omega_q^b + \delta\omega_{\text{colored}}^b \tag{6}$$

where δf_q^b and $\delta\omega_q^b$ represent the acceleration quantization noise vector and angular rate quantization noise vector, respectively. Let δv_q^b and $\delta\alpha_q^b$ denote the delta velocity quantization noise vector and delta angle quantization noise vector, respectively, which are two white noise vectors. Then, the following relationship holds:

$$\delta f_q^b = \delta\dot{v}_q^b \tag{7}$$

$$\delta\omega_q^b = \delta\dot{\alpha}_q^b. \tag{8}$$

Insert (7) and (8) into (5) and (6), and then into (3) and (4), and rearrange the items, and then the following equations can be obtained:

$$\begin{aligned}\delta\dot{v} - C_b^n\delta\dot{v}_q^b = &-\left(\omega_{\text{in}}^n + \omega_{\text{ie}}^n\right) \times \delta v - \psi \times f^b + \delta g^n \\ &+ C_b^n\left(\delta f_{\text{white}}^b + \delta f_{\text{colored}}^b\right)\end{aligned} \tag{9}$$

$$\dot{\psi} - C_b^n\delta\dot{\alpha}_q^b = -\omega_{\text{in}}^n \times \psi + C_b^n\left(\delta\omega_{\text{white}}^b + \delta\omega_{\text{colored}}^b\right). \tag{10}$$

Consider the following relationship:

$$C_b^n\delta\dot{v}_q^b = \dot{\left(C_b^n\delta v_q^b\right)} - \dot{C}_b^n\,\delta v_q^b \tag{11}$$

$$C_b^n\delta\dot{\alpha}_q^b = \dot{\left(C_b^n\delta\alpha_q^b\right)} - \dot{C_b^n}\delta\alpha_q^b \tag{12}$$

then (9) and (10) can be rewritten as

$$\begin{aligned}\delta\dot{v} - \dot{\left(C_b^n\delta v_q^b\right)} = &-\left(\omega_{\text{in}}^n + \omega_{\text{ie}}^n\right) \times \delta v - \psi \times f^b + \delta g^n \\ &+ C_b^n\left(\delta f_{\text{white}}^b + \delta f_{\text{colored}}^b\right) - \dot{C}_b^n\delta v_q^b\end{aligned} \tag{13}$$

$$\begin{aligned}\dot{\psi} - \dot{\left(C_b^n\delta\alpha_q^b\right)} = &-\omega_{\text{in}}^n \times \psi + C_b^n\left(\delta\omega_{\text{white}}^b + \delta\omega_{\text{colored}}^b\right) \\ &- \dot{C}_b^n\delta\alpha_q^b.\end{aligned} \tag{14}$$

According to the left hand sides of (13) and (14), define a new velocity error vector and a new attitude error vector as follows:

$$\delta\hat{v} = \delta v - C_b^n\delta v_q^b \tag{15}$$

$$\hat{\psi} = \psi - C_b^n\delta\alpha_q^b. \tag{16}$$

Substitution of (15) and (16) into (13) and (14) gives

$$\begin{aligned}\delta\dot{\hat{v}} = &-\left(\omega_{\text{in}}^n + \omega_{\text{ie}}^n\right) \times \delta\hat{v} - \hat{\psi} \times f^b + \delta g^n \\ &+ C_b^n\left(\delta f_{\text{white}}^b + \delta f_{\text{colored}}^b\right) - \left(C_b^n\delta\alpha_q^b\right) \times f^b \\ &- \left[\dot{C}_b^n\delta v_q^b + \left(\omega_{\text{in}}^n + \omega_{\text{ie}}^n\right) \times \left(C_b^n\delta v_q^b\right)\right]\end{aligned} \tag{17}$$

$$\begin{aligned}\dot{\hat{\psi}} = &-\omega_{\text{in}}^n \times \hat{\psi} + C_b^n\left(\delta\omega_{\text{white}}^b + \delta\omega_{\text{colored}}^b\right) \\ &- \left[\dot{C}_b^n\delta\alpha_q^b + \omega_{\text{in}}^n \times \left(C_b^n\delta\alpha_q^b\right)\right].\end{aligned} \tag{18}$$

Consider the following relationship:

$$\dot{C}_b^n = C_b^n\left(\omega_{\text{ib}}^b\times\right) - \left(\omega_{\text{in}}^n\times\right)C_b^n \tag{19}$$

and the modified INS error dynamics can be derived as

$$\delta\dot{n} = \delta\hat{v} - \omega_{\text{en}} \times \delta n + \left\{C_b^n\delta v_q^b\right\} \tag{20}$$

$$\begin{aligned}\delta\dot{\hat{v}} = &-\left(\omega_{\text{in}}^n + \omega_{\text{ie}}^n\right) \times \delta\hat{v} - \hat{\psi} \times f^b + \delta g^n \\ &+ C_b^n\left(\delta f_{\text{white}}^b + \delta f_{\text{colored}}^b\right) + \left\{(f^b\times)C_b^n\delta\alpha_q^b\right. \\ &\left. - \left[C_b^n\left(\omega_{\text{ib}}^b\times\right) + \left(\omega_{\text{ie}}^n\times\right)C_b^n\right]\delta v_q^b\right\}\end{aligned} \tag{21}$$

$$\begin{aligned}\dot{\hat{\psi}} = &-\omega_{\text{in}}^n \times \hat{\psi} + C_b^n\left(\delta\omega_{\text{white}}^b + \delta\omega_{\text{colored}}^b\right) \\ &- \left\{C_b^n\left(\omega_{\text{ib}}^b\times\right)\delta\alpha_q^b\right\}.\end{aligned} \tag{22}$$

The quantities in the braces in (20) to (22) are additional white noises arising from quantization noises. They will be used to augment the process noise matrix, Q. To do this, the following theorem should be introduced first.

Theorem A: Given two white noise processes are as follows:

$$w_1(t) = A_1\omega_{10}(t)$$

$$w_2(t) = A_2\omega_{20}(t)$$

where $\omega_{10}(t)$ and $\omega_{20}(t)$ are two unit white noises independent of each other. Define a new stochastic process $v(t)$ as

$$v(t) = w_1(t) + w_2(t).$$

Then, $v(t)$ is also a white noise with a power spectral density (PSD) A^2 as

$$A^2 = A_1^2 + A_2^2.$$

TABLE I
THE ORIGINAL AND AUGMENTED DRIVING WHITE NOISES OF INS ERROR DYNAMICS

	Original Driving White Noise	Augmented Driving White Noise
Position Error Dynamics	0	$C_b^n \delta v_q^b$
Velocity Error Dynamics	$C_b^n \delta f_{white}^b$	$C_b^n \delta f_{white}^b + (f^b\times) C_b^n \delta\alpha_q^b - [C_b^n(\omega_{ib}^b\times) + (\omega_{ie}^n\times) C_b^n]\delta v_q^b$
Attitude Error Dynamics	$C_b^n \delta\omega_{white}^b$	$C_b^n \delta\omega_{white}^b - C_b^n(\omega_{ib}^b\times)\delta\alpha_q^b$

This theorem can be easily proved according to the definition of white noise [31], and can also be easily extended to the situation of multiple white noises.

According to (7) and (8), the following relationship about PSDs can be obtained [32]:

$$S_q(j\omega) = \omega^2 S_w(j\omega) \tag{23}$$

where $S_q(j\omega)$ represents the PSD of quantization noise δf_q^b or $\delta\omega_q^b$, and $S_w(j\omega)$ represents the PSD of driving white noise δv_q^b or $\delta\alpha_q^b$. According to [21], the PSD of quantization noise has the following form:

$$S_q(j\omega) = \omega^2 q^2 T \tag{24}$$

where q is the parameter of quantization noise that can be determined by using the Allan Variance analysis [21], and T is the sampling interval. So, the PSD of driving white noise can be computed from (23) and (24) as follows:

$$S_w(j\omega) = q^2 T. \tag{25}$$

So, according to (25), the PSDs of δv_q^b and $\delta\alpha_q^b$ can be written as

$$S_v(j\omega) = q_v^2 T \tag{26}$$

$$S_\alpha(j\omega) = q_\alpha^2 T \tag{27}$$

where q_v and q_α can be determined from the Allan Variance analysis to accelerometers and gyros, respectively.

According to (2) to (4) and (20) to (22), the original driving white noises and the augmented driving white noises of the INS error equations are listed in Table I, where the PSDs of $\delta f_{\text{white}}^b$ and $\delta\omega_{\text{white}}^b$ can be obtained from the Allan Variance analysis, and the PSDs of δv_q^b and $\delta\alpha_q^b$ can be determined according to (26) and (27). So the PSDs of the augmented driving white noises listed in Table I can be computed according to Theorem A. Given the PSDs of the augmented driving white noises, the augmented process noise matrix, Q, can be easily determined according to the method discussed in [27].

III. MODELING AND PROCESSING OF THE COLORED NOISES

In this section, the colored noises will be modeled and the obtained model will be used to augment the Kalman Filter for GPS/INS integration. Multiple colored noises, such as, bias instability, random walk, or ramp noise, may concurrently exist in an inertial sensor. The differential equation descriptions for each of these colored noises will be derived first. Then, the equivalent representation of these differential equations will be deduced. Finally, the equivalent representation for the multiple colored noises will be used to augment the Kalman Filter for GPS/INS integration.

A. Differential Equation Descriptions of the Colored Noises

As mentioned in Section I, the PSDs of the colored noises can be obtained by means of the Allan Variance analysis. In this subsection, a technique will be presented to derive the differential equation descriptions of the colored noises from the obtained PSDs.

According to [27], a stochastic error with a specific PSD can be generated by passing a unit white noise through a predesigned shaping filter. On the contrary, if the PSD of a stochastic error is given, the shaping filter can also be derived. According to different forms of the shaping filters, the differential equation descriptions of the stochastic errors can be obtained by different approaches. If the transfer function of the shaping filter is rational, the differential equation can be directly derived according to the approach in [27]. Otherwise, a technique is first proposed to obtain the rational approximation of the transfer function, and then the differential equation is derived from the approximated transfer function. In the remaining part of this subsection, the differential equation descriptions for the random walk, the bias instability, and the ramp noise will be derived one by one.

The random walk has a rational spectrum, so the transfer function of the corresponding shaping filter, $G(j\omega)$, is a rational function and the corresponding differential equation description can be directly derived according to the approach in [27]. According to [21], the PSD of the random walk is

$$S_{\text{rw}}(\omega) = K^2/\omega^2. \tag{28}$$

According to [27], the transfer function of the corresponding shaping filter can be written as

$$G_{\text{rw}}(j\omega) = K/j\omega. \tag{29}$$

Carry out the inverse Fourier transform in both sides of (29), and then the differential equation description for the random walk can be formulated as

$$\dot{d}_{\text{rw}}(t) = K u_1(t) \tag{30}$$

where $u_1(t)$ is a unit white noise.

The bias instability and the ramp noise have irrational spectra, so the transfer functions of the corresponding shaping filters are irrational functions. Rational approximations should be made according to the above analysis. Then, the approximate and true transfer functions will be compared with each other to assess the errors introduced by the approximation.

According to [21], the PSD of the bias instability is rewritten as follows:

$$S_{\text{fn}}(\omega) = B^2/\omega. \tag{31}$$

According to [27], the true transfer function of the corresponding shaping filter for the bias instability can be written as

$$G_{\rm fn}(j\omega) = B/\sqrt{j\omega}. \tag{32}$$

Perform Taylor series expansion for $\sqrt{j\omega}$, and keep the first two terms, and then the approximate transfer function can be written as

$$\hat{G}_{\rm fn}(j\omega) = \beta B/(j\omega + \beta) \tag{33}$$

where β relies on the expanding point of the Taylor series, and will be determined later according to the error analysis of this approximation. Carry out the inverse Fourier transform in both sides of (33), and formulate the differential equation description of the bias instability as follows:

$$\dot{d}_{\rm fn}(t) + \beta d_{\rm fn}(t) = \beta B u_2(t). \tag{34}$$

Actually, (34) represents a first-order Gaussian–Markov process, and this means that, herein, the flicker noise is approximated by a first-order Gaussian–Markov process. The relative magnitude error, in the unit of dB, between $G_{\rm fn}(j\omega)$ and $\hat{G}_{\rm fn}(j\omega)$ can be calculated as

$$\varepsilon_{\rm fn} = 10 * \log |(|\hat{G}_{\rm fn}(j\omega)| - |G_{\rm fn}(j\omega)|)/|G_{\rm fn}(j\omega)||. \tag{35}$$

Insert (32) and (33) into (35), and then the magnitude error can be calculated as

$$\varepsilon_{\rm fn} = 10 * \log |\sqrt{\omega}/\sqrt{1 + \omega^2/\beta^2} - 1|. \tag{36}$$

From (36), it can be found that the relative magnitude error $\varepsilon_{\rm fn}$ is smaller than 0 dB in the whole frequency scope. Considering the low frequency nature of flicker noise, if β is chosen to be 3.97 Hz, the relative magnitude error will be smaller than -3 dB in the frequency band [0.1 Hz, 10 Hz].

A similar procedure can be carried out for the ramp noise, and the true and approximate transfer function can be obtained as follows:

$$G_{\rm rn}(j\omega) = R/(j\omega)^{1.5} \tag{37}$$

$$\hat{G}_{\rm rn}(j\omega) = R/\left(-\omega^2 + j\sqrt{2}\omega_0\omega + \omega_0^2\right). \tag{38}$$

A small difference is that, herein, a three-term Taylor series expansion is performed for $(j\omega)^{1.5}$ to derive the approximate transfer function. Then, the differential equation for the ramp noise can be derived from (38) as follows:

$$\ddot{d}_{\rm rn}(t) + \sqrt{2}\omega_0\dot{d}_{\rm rn}(t) + \omega_0^2 d_{\rm rn}(t) = R u_3(t). \tag{39}$$

It can be easily noted that (39) represents a second-order Gaussian–Markov process. The relative magnitude error, in the unit of dB, between $G_{\rm rn}(j\omega)$ and $\hat{G}_{\rm rn}(j\omega)$ can be calculated as follows:

$$\varepsilon_{\rm rn} = 10 * \log \left| \sqrt{\omega^3}/\sqrt{\omega^4 + \omega_0^4} - 1 \right|. \tag{40}$$

From (40), it can be found that the relative magnitude error $\varepsilon_{\rm rn}$ is also smaller than 0 dB in the whole frequency scope. Considering the ramp noise is also a low frequency noise, if ω_0 is chosen to be 0.01 rad/s, the relative magnitude error $\varepsilon_{\rm rn}$ will be smaller than -0.5 dB in the frequency band [0.1 Hz, 10 Hz].

Until now, the differential equation descriptions of the random walk, the flicker noise and the ramp noise have been obtained and formulated in (30), (34), and (39), respectively.

B. Equivalent Representation of Multiple Colored Noises

In this subsection, the equivalent differential equation representation of multiple colored noises in an inertial sensor will be derived according to the differential equations obtained in the previous subsection. The three noises, namely, the bias instability, the random walk, and the ramp noise, may or may not concurrently exist in the same sensor, which should be determined by the Allan Variance analysis. Herein, the most complicated case, where all these three noises concurrently exist in the same sensor, will be discussed.

The differential equation descriptions of the random walk, the bias instability, and the ramp noise are formulated in (30), (34), and (39), respectively, and herein they are rewritten and transformed by using the differential operator D for convenience

$$d_{\rm rw}(t) = K u_1(t)/D \tag{41}$$

$$d_{\rm fn}(t) = \beta B u_2(t)/(D + \beta) \tag{42}$$

$$d_{\rm rn}(t) = R u_3(t)/\left(D^2 + \sqrt{2}\omega_0 D + \omega_0^2\right). \tag{43}$$

Define a new process $z(t)$ as follows:

$$z(t) = d_{\rm rw}(t) + d_{\rm fn}(t) + d_{\rm rr}(t). \tag{44}$$

Insert (41) to (43) into (44) and rearrange the items, and then the following differential equation can be obtained:

$$\begin{aligned} &D(D+\beta)\left(D^2 + \sqrt{2}\omega_0 D + \omega_0^2\right) z(t) \\ &\quad = (D+\beta)(D^2 + \sqrt{2}\omega_0 D + \omega_0^2) K u_1(t) \\ &\qquad + D\left(D^2 + \sqrt{2}\omega_0 D + \omega_0^2\right)\beta B u_2(t) \\ &\qquad + D(D+\beta) R u_3(t). \end{aligned} \tag{45}$$

The left-hand side of (45) can be expanded as

$$z^{(4)}(t) + a_1 z^{(3)}(t) + a_2 z^{(2)}(t) + a_3 z^{(1)}(t) + a_4 z^{(0)}(t) \tag{46}$$

where the superscripts in the parentheses represent the orders of derivatives, and the coefficients can be computed as follows:

$$\begin{aligned} a_1 &= \beta + \sqrt{2}\omega_0 \\ a_2 &= \sqrt{2}\omega_0\beta + \omega_0^2 \\ a_3 &= \beta\omega_0^2 \\ a_4 &= 0. \end{aligned}$$

Let the right-hand side of (45) equal to a new stochastic process $s(t)$, and obtain

$$\begin{aligned} s(t) = (D+\beta)\left(D^2+\sqrt{2}\omega_0 D+\omega_0^2\right)Ku_1(t) \\ + D(D^2+\sqrt{2}\omega_0 D+\omega_0^2)\beta B u_2(t) \\ + D(D+\beta)Ru_3(t). \end{aligned} \quad (47)$$

It can be found that $s(t)$ is a stochastic process driven by three independent unit white noises.

Define another stochastic process $s'(t)$ as follows:

$$s'(t) = b_0\omega^{(3)}(t) + b_1\omega^{(2)}(t) + b_2\omega^{(1)}(t) + b_3\omega^{(0)}(t) \quad (48)$$

where $\omega(t)$ is a unit white noise, and the coefficients are defined as follows:

$$\begin{aligned} b_0^2 &= K^2+\beta^2B^2 \\ b_1^2 - 2b_0b_2 &= K^2\beta^2+R^2 \\ b_2^2 - 2b_1b_3 &= K^2\omega_0^4+\beta^2B^2\omega_0^4+\beta^2R^2 \\ b_3^2 &= K^2\beta^2\omega_0^4. \end{aligned}$$

It can be easily proven that the following relationship holds:

$$\begin{aligned} &E[s'(t)] \\ &\quad = E[s(t)] = 0 \end{aligned} \quad (49)$$

$$\begin{aligned} &E[s'(t)s'(t-\tau)] \\ &\quad = E[s(t)s(t-\tau)] \\ &\quad = -(K^2+\beta^2B^2)\delta^{(6)}(\tau) + (K^2\beta^2+R^2)\delta^{(4)}(\tau) \\ &\qquad - (K^2\omega_0^4+\beta^2B^2\omega_0^4+\beta^2R^2)\delta^{(2)}(\tau) + K^2\beta^2\omega_0^4\delta(\tau). \end{aligned} \quad (50)$$

The above two equations demonstrate that $s'(t)$ and $s(t)$ are equivalent in terms of wide sense stationarity (WSS). As is known, the Kalman Filter only requires the PSDs of the driving noises. Because $s'(t)$ and $s(t)$ are equivalent in terms of WSS, they will have the same autocorrelation function and PSD. So, the equivalence in terms of WSS is enough for Kalman Filtering applications.

Insert (46) and (48) into (45), the equivalent differential equation representation of the hybrid of the random walk, the flicker noise, and the ramp noise can be obtained as follows:

$$\begin{aligned} z^{(4)}(t) + a_1z^{(3)}(t) + a_2z^{(2)}(t) + a_3z^{(1)}(t) + a_4z^{(0)}(t) \\ = b_0\omega^{(3)}(t) + b_1\omega^{(2)}(t) + b_2\omega^{(1)}(t) + b_3\omega^{(0)}(t) \end{aligned} \quad (51)$$

which is a four-order differential equation driven by a unit white noise. Equation (51) can be used to augment the Kalman Filter for GPS/INS integration to precisely estimate and compensate the stochastic errors in inertial sensors.

C. Augmenting the Kalman Filter for GPS/INS Integration

In this subsection, the state-space equation and process noise covariance matrix of Kalman Filter for GPS/INS integration is augmented by using the equivalent representation of multiple colored noises in inertial sensors. The processing procedure is shown in Fig. 3.

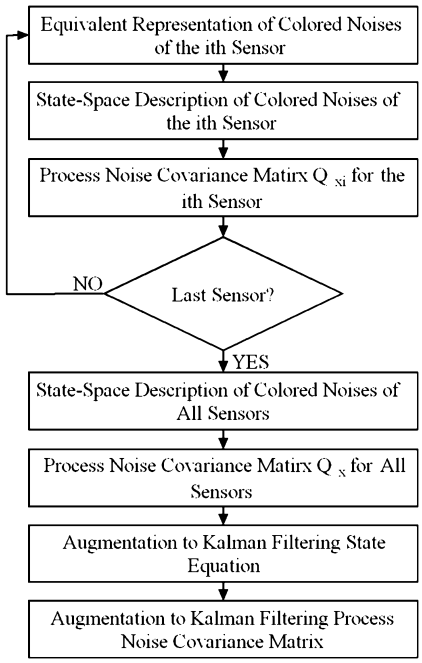

Fig. 3. The flowchart of using the equivalent representation of multiple colored noises in inertial sensors to augment GPS/INS integration.

The state-space equation of Kalman Filter for GPS/INS integration can be derived from (20) to (22) as follows:

$$\dot{Y}(t) = F_{YY}(t)Y(t) + E(t) \quad (52)$$

where $F_{YY}(t)$ is the system matrix, and $Y(t)$ is the state vector composed of position errors, velocity errors, attitude errors, gravity errors, and lever-arm errors, and can be expressed as follows [12]:

$$Y(t) = [\delta n^T \;\; \delta\hat{v}^T \;\; \hat{\psi}^T \;\; \delta g^T \;\; \delta l^T]^T. \quad (53)$$

In (52), $E(t)$ is a stochastic error vector and can be divided into two parts

$$E(t) = \omega_Y(t) + Z(t) \quad (54)$$

where $\omega_Y(t)$ is the white noise part, which accounts for the common white noise and the equivalent white noise derived from the quantization noise, and $Z(t)$ is the colored noise part, which accounts for the bias instability, the random walk and the ramp noise. The white noise part, $\omega_Y(t)$, is used to compute the initial process noise covariance matrix of system, and the colored noise part will be used to augment the Kalman Filter of GPS/INS integration.

From (20) and (22), it is noted that the colored noises only exist in the velocity error equation (21) and attitude error equation (22), so $Z(t)$ can be formulated as follows:

$$Z(t) = [0_{1\times3} \quad z_1(t) \quad \cdots \quad z_6(t) \quad 0_{1\times6}]^T \quad (55)$$

where $z_i(t), i = 1,\ldots,3$ represents the stochastic errors in the ith accelerometer, and $z_i(t), i = 4,\ldots,6$ represents the stochastic errors in the ith gyros. Because $z_i(t)$ accounts for the

hybrid effect of the bias instability, the random walk, and the ramp noise in an inertial sensor, it satisfies (51)

$$z_i^{(4)}(t) + a_1 z_i^{(3)}(t) + a_2 z_i^{(2)}(t) + a_3 z_i^{(1)}(t) + a_4 z_i^{(0)}(t) = b_0 \omega_i^{(3)}(t) + b_1 \omega_i^{(2)}(t) + b_2 \omega_i^{(1)}(t) + b_3 \omega_i^{(0)}(t) \quad (56)$$

where $z_i(t)$ represents the equivalent representation of the multiple colored noises, and $\omega_i(t)$ is the equivalent driving white noise, and the superscripts in the parentheses represent the orders of derivatives.

In the following part of this section, the state-space description of $z_i(t)$ is derived according to the state-space realization of (56), and then the state-space description of $Z(t)$ is obtained by combining the state-space descriptions for all sensors, and finally the system state-space equation is augmented by using the state-space description of $Z(t)$.

The state-space description of $z_i(t)$ can be obtained by using the following approach. According to [33], the state-space realization of (56) can be expressed as follows:

$$\dot{x}_i(t) = F_i x_i(t) + G_i \omega_i(t) \quad (57)$$

$$z_i(t) = H_i x_i(t) \quad (58)$$

where $x_i(t)$ is a four-dimension state vector, $\omega_i(t)$ is a unit white noise, and F_i, G_i and H_i are derived from the coefficients of (56), and are expressed as follows:

$$F_i = \begin{bmatrix} 0 & 0 & 0 & -a_4 \\ 1 & 0 & 0 & -a_3 \\ 0 & 1 & 0 & -a_2 \\ 0 & 0 & 1 & -a_1 \end{bmatrix}, \quad G_i = \begin{bmatrix} b_3 \\ b_2 \\ b_1 \\ b_0 \end{bmatrix}, \quad H_i = \begin{bmatrix} 0 \\ 0 \\ 0 \\ 1 \end{bmatrix}^T.$$

According to the above expressions for F_i, G_i and H_i, (57) and (58) are the observable canonical form realization of (56). Observable canonical form means that the state vector $x_i(t)$ is completely observable with the knowledge of $z_i(t)$, which is a preferable property in state estimation.

The process noise covariance matrix, Q_{x_i}, of (57) is required in Kalman Filtering, and can be computed as follows:

$$E[(G_1\omega_i(t))(G_1\omega_i(t-\tau))^T] = Q_{x_i}\delta(\tau). \quad (59)$$

Considering the fact that $\omega_i(t)$ is a unit white noise, Q_{x_i} can be obtained by inserting G_i into (59)

$$Q_{x_i} = \begin{bmatrix} b_3^2 & b_3b_2 & b_3b_1 & b_3b_0 \\ b_2b_3 & b_2^2 & b_2b_1 & b_2b_0 \\ b_1b_3 & b_1b_2 & b_1^2 & b_1b_0 \\ b_0b_3 & b_0b_2 & b_0b_1 & b_0^2 \end{bmatrix}. \quad (60)$$

The state-space description of $Z(t)$ can be obtained by combining the state-space descriptions of all the $z_i(t)s$ for all sensors

$$\dot{X}(t) = F_{XX}(t)X(t) + \omega_X(t) \quad (61)$$

$$Z(t) = H(t)X(t) \quad (62)$$

where $Z(t)$ has been formulated in (55), and $X(t)$ is a 24-dimension state vector formulated as follows:

$$X(t) = [x_1^T(t) \quad \cdots \quad x_6^T(t)]^T.$$

TABLE II
THE NOISE PARAMETERS OF INERTIAL SENSORS FROM THE MANUAL

Noise Type	Noise Para.(unit)	Gyro	Acce.
Quantization Noise	Q(rad or m/s)	5.000e-6	2.000e-4
White Noise	N(rad/ $s^{0.5}$ or m/ $s^{1.5}$)	1.018e-5	5.868e-4
Bias Instability	B(rad/s or m/ s^2)	2.424e-5	4.900e-3

Other quantities in (61) and (62) can be derived as follows:

$$F_{XX}(t) = \mathrm{diag}(F_1, \ldots, F_6)$$
$$\omega_X(t) = [G_1^T\omega_1(t) \cdots G_6^T\omega_6(t)]^T$$
$$H(t) = [0_{24\times3}\ \hat{H}^T\ 0_{24\times6}]^T$$

where $\hat{H}$ is defined as

$$\hat{H} = \mathrm{diag}(H_1 \quad H_2 \quad \cdots \quad H_6).$$

The process noise covariance matrix of (61) can be obtained by using the same method as in (59) and by considering the fact that the driving noises are independent with each other

$$Q_X = \mathrm{diag}(Q_1 \quad \cdots \quad Q_6). \quad (63)$$

The augmented system state-space equation can be obtained by (52), (54), (61), and (62)

$$\begin{bmatrix} \dot{Y}(t) \\ \dot{X}(t) \end{bmatrix} = \begin{bmatrix} F_{YY}(t) & F_{XY}(t) \\ 0 & F_{XX}(t) \end{bmatrix} \begin{bmatrix} Y(t) \\ X(t) \end{bmatrix} + \begin{bmatrix} \omega_Y(t) \\ \omega_X(t) \end{bmatrix} \quad (64)$$

where $F_{YY}(t)$ is the original system matrix, and $F_{XX}(t)$ is the augmenting system matrix, and $F_{XY}(t)$ is equal to $H(t)$ in (62).

The process noise covariance matrix of (64) can also be obtained by using the same method as in (59) and by considering the fact that the driving noises are independent with each other

$$Q = \begin{bmatrix} Q_Y & 0_{15\times24} \\ 0_{24\times15} & Q_X \end{bmatrix} \quad (65)$$

where Q_Y is the original process noise covariance matrix, and Q_X is the augmenting process noise covariance matrix.

IV. EXPERIMENTAL TESTS

In this section, the proposed stochastic error modeling scheme for inertial sensors shown in Fig. 2 was applied to an integrated GPS/INS system, and the system performance was evaluated in field tests.

CMIGITS-II, an integrated GPS/INS system developed by Boeing, was used to collect data in our research. The IMU of CMIGITS-II is composed of three micromachined quartz gyros and three vibrating quartz accelerometers, and the stochastic error characteristics provided by the user manual [34] are listed in Table II, where the noise parameters for random walk and ramp noise are not provided by the manual.

At the first stage, CMIGITS-II was used to collect static data up to six hours. Allan Variance analysis was applied to the static data to analyze the stochastic error sources existing in the inertial sensors and to determine the corresponding noise parameters.

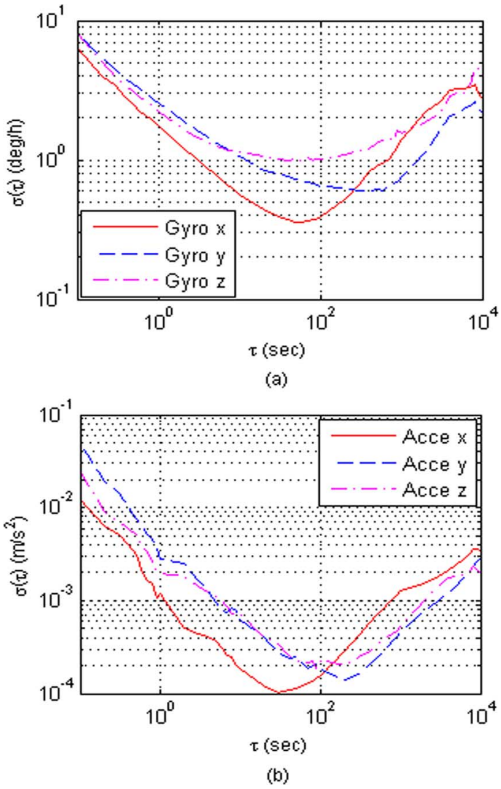

Fig. 4. Root Allan Variance plots for (a) gyros in x, y, and z axes, and (b) accelerometers in x, y, and z axes. Both the gyros and accelerometers have a sampling rate of 100 Hz.

At the second stage, CMIGITS-II was operated in a field test and the dynamic data was collected. A loosely coupled integration of GPS/INS was implemented in postprocessing mode. During the postprocessing, the conventional stochastic error modeling approach shown in Fig. 1 and the proposed stochastic error modeling approach shown in Fig. 2 were applied respectively to the Kalman Filtering of GPS/INS integration. The performances of these two approaches were compared from two levels: the input of the navigation system and the output of the navigation system. At the input level, the inertial sensor drift estimates from these two approaches were compared. At the output level, the navigation errors from these two approaches were compared.

A. Allan Variance Analysis to the Inertial Sensors Used

The techniques of the Allan Variance analysis has been discussed in [11], [21], and [23]–[26]. The results of the Allan Variance analysis are presented in Fig. 4, which is a log-log plot of the root Allan Variance, $\sigma(\tau)$, relative to the correlation time τ. According to [21], different noises have different slopes in the log-log plot of Allan Variance. So, from Fig. 4, it can be noted that quantization noise and ramp noise are not significant in the tested gyros, and ramp noise is not significant in the tested accelerometers.

The noise parameters of the inertial sensors can also be determined from Allan Variance analysis by using lest squares fitting [25] and the results are listed in Table III for gyros and in Table IV for accelerometers.

TABLE III
THE NOISE PARAMETERS OF GYROS DERIVED BY ALLAN VARIANCE ANALYSIS

Noise Type	Noise Para.(unit)	Gyro x	Gyro y	Gyro z
Quantization Noise	Q(rad)	9.245e-8	8.304e-8	5.512e-8
White Noise	N(rad/ $s^{0.5}$)	0.871e-5	1.239e-5	1.695e-5
Bias Instability	B(rad/s)	2.701e-6	4.931e-6	7.856e-6
Random Walk	K(rad/ $s^{1.5}$)	4.135e-7	3.473e-7	2.551e-7
Ramp Noise	R(rad/ s^2)	0	0	0

TABLE IV
THE NOISE PARAMETERS OF ACCELEROMETERS DERIVED BY ALLAN VARIANCE ANALYSIS

Noise Type	Noise Para.(unit)	Acce. x	Acce. y	Acce. z
Quantization Noise	Q(m/s)	9.1086e-4	6.2041e-3	2.8567e-3
White Noise	N(m/ $s^{1.5}$)	4.1018e-3	1.1306e-4	2.1094e-3
Bias Instability	B(m/ s^2)	1.2279e-4	1.7344e-4	2.0132e-4
Random Walk	K(m/ $s^{2.5}$)	3.1169e-5	1.4250e-5	2.0382e-5
Ramp Noise	R(m/ s^3)	2.1354e-8	4.2902e-8	1.6184e-8

According to the noise parameters determined above, the white noise was used to obtain the initial process noise covariance matrix, Q, and the quantization noise was used to augment the Q matrix by using the approach proposed in Section II. Then, the differential equation descriptions of the colored noises were obtained by following the approach proposed in Section III-A. Then, the equivalent representation of the multiple colored noises was derived according to Section III-B. Finally, this derived equivalent representation was used to augment the Kalman Filter for GPS/INS integration according to Section III-C.

B. Dynamic Performance Analysis

The performances of the conventional stochastic error modeling approach and the proposed approach were compared during postprocessing. The system was first operated in the GPS/INS integration mode, and then when the stable navigation solutions were output, the GPS signal was cut off for 2 min and the system was operated in the free INS mode during this period. In the integration mode, the drifts of the inertial sensors were continuously estimated. In the free INS mode, the estimated drifts of the inertial sensors were applied to the inertial computation to compensate the errors of the inertial sensors, and the navigation errors of the free INS greatly depends on the accuracy of the estimated drifts of the inertial sensors. The same process was carried out twice, and the conventional model and the proposed model were applied, respectively.

The proposed model can account for all the possible stochastic errors in inertial sensors, while the conventional model can only account for white noise and random walk, so it is expected that the proposed model can estimate the drifts of the inertial sensors more precisely during the integration Kalman Filtering. In our Kalman Filtering design for GPS/INS integration, the drifts of the inertial sensors are estimated and compensated consecutively, namely, in the first filtering cycle, the

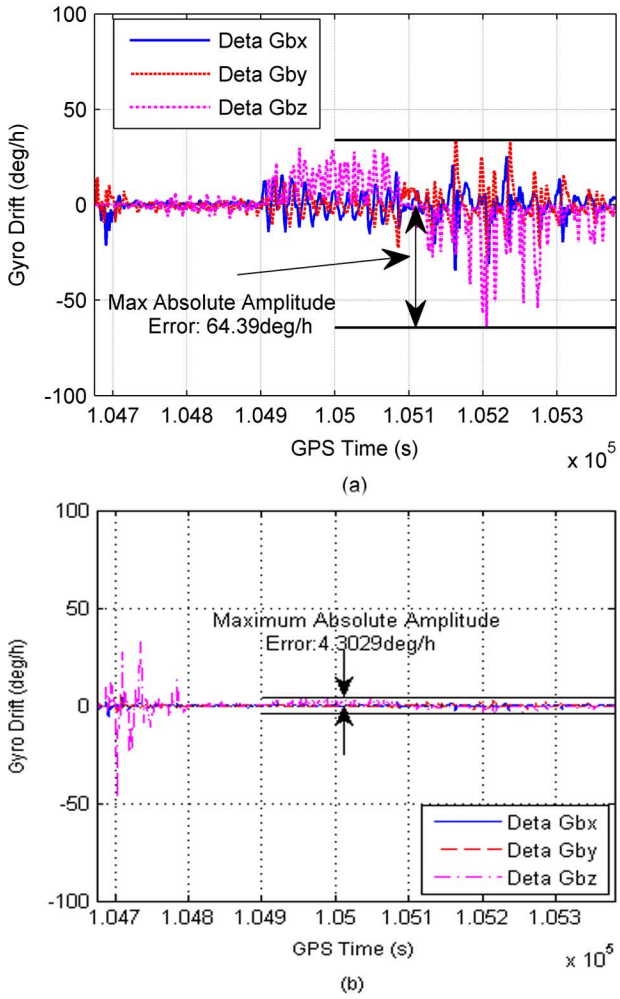

Fig. 5. Estimated drifts of gyros using (a) the conventional modeling approach and (b) the proposed modeling approach.

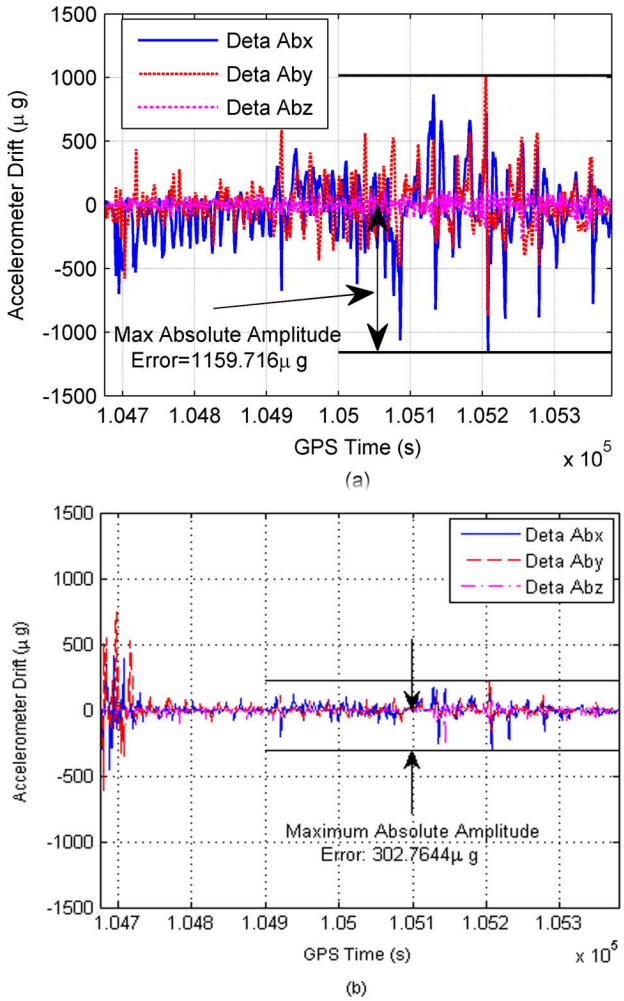

Fig. 6. Estimated drifts of accelerometers using (a) the conventional modeling approach and (b) the proposed modeling approach.

drifts are estimated and compensated, and in the next filtering cycle, the residual drifts are estimated and compensated, and so on. So, after the consecutive compensation, the estimated drifts from the proposed model should converge to smaller values than those from the conventional model.

Figs. 5 and 6 shows the estimated drifts of gyros and accelerometers, respectively, by using both the conventional modeling approach and the proposed modeling approach. It can be noted that the maximum absolute amplitude error of the gyros' drifts estimation by using the conventional approach is almost 15 times larger than that by using the proposed approach, and this figure is almost four times larger for the accelerometers.

With the DGPS solutions as the reference, the navigation results for these two models are compared in Figs. 7 and 8. From Fig. 7, it can be noted that the horizontal position error is 325.5 m after the 2-min free INS operation using the conventional model, while it is 80.9 m by using the proposed model. The horizontal position error is reduced by 75.1% during this operation. Fig. 8 shows the changes of east displacement, north displacement, and height with GPS time. Before GPS time 105400s, the system is operated in the GPS/INS integration mode, and from GPS time 105400–105520 s, the GPS signals are cut off and the INS is operated in the free mode. It can

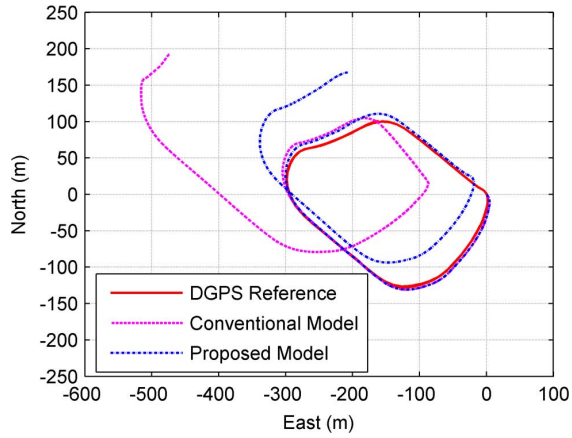

Fig. 7. Trajectory comparison among the DGPS reference, the solution from the conventional model, and the solution from the proposed model.

be noted that, after the 2-min GPS signals outages, the east displacement error is 312.5 m by using the conventional model and 45.6 m by using the proposed model; the north displacement error is −91.2 m by using the conventional model and −66.9 m by using the proposed model; and the height error is −8.1 m by using the conventional model and −6.7 m by

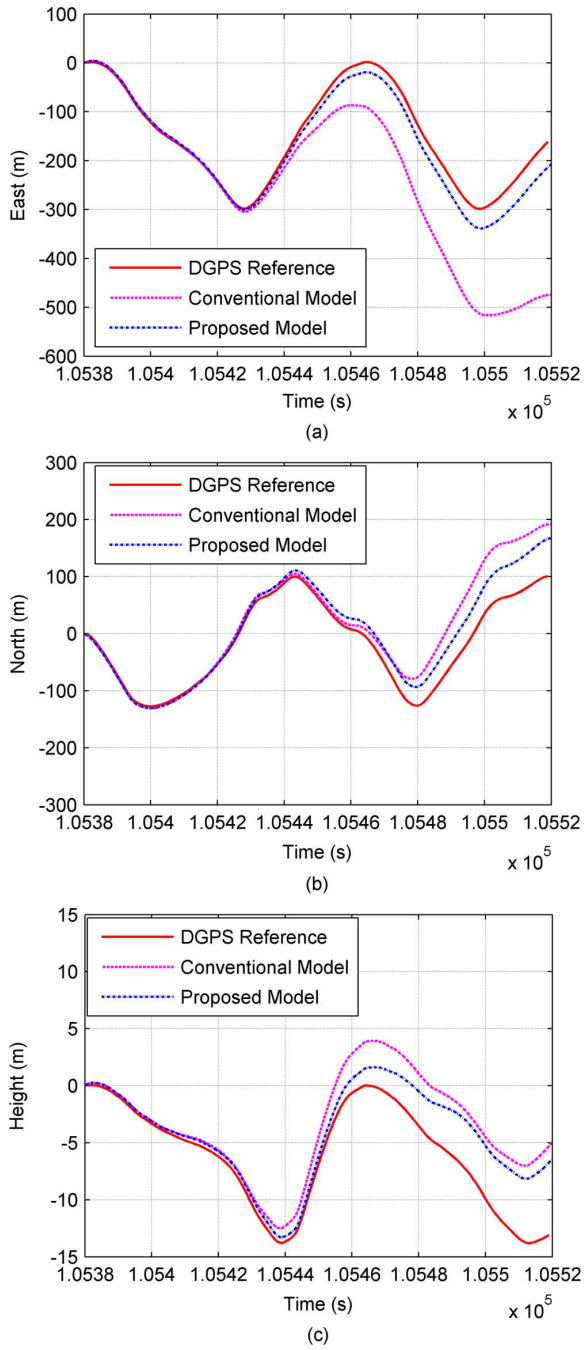

Fig. 8. (a) East Displacement, (b) North Displacement, and (c) Height comparison among the DGPS reference, the solution from the conventional model, and the solution from the proposed model.

using the proposed model. The east displacement error, north displacement error, and height error are improved 85.4%, 26.6%, and 17.3%, respectively.

Furthermore, it can be noted that the application of this new stochastic error model will increase the dimensions of the system matrix, but considering the ever increasing computing power, this might not be a concern. For example, our PC processor can process the data collected for 20 min in about 3 min. Therefore, the 1 Hz Kalman Filtering update only needs 0.15 s, which is sufficient for many real-time applications.

V. Concluding Remarks

In this paper, a stochastic error modeling approach for inertial sensors has been proposed, and its applications in GPS/INS integration have been discussed. Specifically, the following tasks have been completed.

- A modified INS error dynamics has been developed to model the quantization noise.
- The hybrid of multiple colored noises has been modeled by using an equivalent differential equation, and a technique has been proposed to augment the Kalman Filter of GPS/INS integration by using this equivalent differential equation.
- The performance of this proposed stochastic error modeling approach for the inertial sensors has been demonstrated in GPS/INS integration applications.

References

[1] P. D. Groves, *Principles of GNSS, Inertial, and Multisensor Integrated Navigation Systems*. Norwood, MA: Artech House, 2008, p. 363.
[2] A. A. Morgan, "Calibration of an inertial sensor system," U.S. Patent 5 421 187, Jun. 6, 1995.
[3] A. S. Oravetz and H. J. Sandberg, "Stationary and nonstationary characteristic of gyro drift rate," *AIAA J.*, vol. 8, no. 10, pp. 1765–1766, 1970.
[4] S. M. Pandit and W. Zhang, "Modeling random gyro drift rate by data dependent systems," *IEEE Trans. Aerosp. Electron. Syst.*, vol. 22, no. 4, pp. 455–460, Jul. 1986.
[5] S. Nassar, K. P. Schwarz, A. Noureldin, and N. El-Sheimy, "Modeling inertial sensor errors using autoregressive (AR) models," in *Proc. ION NTM 2003*, Anaheim, CA, 2003, pp. 116–125.
[6] S. Nassar, K. P. Schwarz, and N. El-Sheimy, "INS and INS/GPS accuracy improvement using autoregressive (AR) modeling of INS sensor errors," in *Proc. ION NTM 2004*, San Diego, CA, 2004, pp. 936–944.
[7] R. L. Hammon, "An application of random process theory to gyro drift analysis," *IRE Trans. Aeronaut. Nav. Electron.*, vol. 7, no. 3, pp. 84–91, Sep. 1960.
[8] R. L. Hammon, "Effects on inertial guidance systems of random error sources," *IRE Trans. Aeronaut. Nav. Electron*, vol. 9, no. 4, pp. 215–230, Dec. 1962.
[9] B. Danik, "The least-square approximation of inertial platform drift," *IEEE Trans. Aerosp. Electron. Syst.*, vol. 2, no. 5, pp. 591–594, Sep. 1966.
[10] K. P. Schwarz and M. Wei, "INS/GPS integration for geomatics," Dept. Geomatics Engineering, Univ. Calgary. Calgary, AB, Canada, pp. 34–42, 2001.
[11] J. Wang, H. K. Lee, S. Hewitson, and H. K. Lee, "Influence of dynamics and trajectory on integrated GPS/INS navigation performance," *J. Global Positioning Syst.*, vol. 2, no. 2, pp. 109–116, Dec. 2003.
[12] H. Kim, J. G. Lee, and C. G. Park, "Performance improvement of GPS/INS integrated system using Allan Variance analysis," in *Proc. Int. Symp. GPS/GNSS 2004*, Sydney, Australia, 2004.
[13] D. Grejner-Brzezinska, C. Toth, and Y. Yi, "On improving navigation accuracy of GPS/INS systems," *Photogrammetric Engineering Remote Sensing*, vol. 71, no. 4, pp. 377–389, Apr. 2005.
[14] S. Han and J. Wang, "Monitoring the degree of observability in integrated GPS/INS systems," in *Proc. Int. Symp. GPS/GNSS 2008*, Tokyo, Japan, 2008, pp. 414–421.
[15] Y. Yi, "On improving the accuracy and reliability of GPS/INS-based direct sensor georeferencing," Ph.D. dissertation, Dept. Geodetic Science and Surveying, Ohio State Univ., Columbus, OH, 2007, pp. 102..
[16] *IEEE Standard Specification Format Guide and Test Procedure for Single-Axis Interferometric Fiber Optic Gyros*, IEEE Standard 952, 1997, pp. 62–73.
[17] A. Dushman, "On gyro drift models and their evaluation," *IRE Trans. Aeronaut. Nav. Electron.*, vol. 9, no. 4, pp. 230–234, Dec. 1962.
[18] S. Nassar and N. El-Sheimy, "A combined algorithm of improving INS error modeling and sensor measurements for accurate INS/GPS navigation," *GPS Solutions*, vol. 10, no. 1, pp. 29–39, Jul. 2006.
[19] H. J. Lee and S. Jung, "Gyro sensor drift compensation by Kalman filter to control a mobile inverted pendulum robot system," in *Proc. IEEE Conf. Ind. Technol.*, Gippsland, Australia, 2009, pp. 1–6.

[20] D. W. Allan, "Statistics of atomic frequency standards," *Proc. IEEE*, vol. 54, no. 2, pp. 221–230, Feb. 1966.
[21] *IEEE Standard Specification Format Guide and Test Procedure for Single-Axis Laser Gyros*, IEEE Standard 647, 2006, pp. 74.
[22] H. Hou and N. El-Sheimy, "Inertial sensors errors modeling using Allan Variance," in *Proc. ION GPS/GNSS 2003*, Portland, OR, 2003, pp. 2860–2867.
[23] N. El-Sheimy, H. Hou, and X. Niu, "Analysis and modeling of inertial sensors using Allan Variance," *IEEE Trans. Instrum. Meas.*, vol. 57, no. 1, pp. 140–149, Jan. 2008.
[24] M. M. Tehrani, "Ring laser gyro data analysis with cluster sampling technique," in *Proc. Fiber Optics and Laser Sensors*, Arlington, VA, 1983, pp. 207–220.
[25] L. C. Ng, "On the application of Allan Variance method for ring laser gyro performance characterization," Lawrence Livermore National Lab., Livermore, CA, Rep. No. UCRL-ID-115695, 1993.
[26] L. C. Ng and D. J. Pines, "Characterization of ring laser gyro performance using the Allan Variance method," *J. Guidance, Control, and Dynamics*, vol. 20, no. 1, pp. 211–214, Jan. 1997.
[27] R. G. Brown and P. Y. C. Hwang, *Introduction to Random Signals and Applied Kalman Filtering*, 3rd ed. New York: Wiley, 1997, pp. 193, 225–228, 290.
[28] P. G. Savage, "Analytical modeling of sensor quantization in strapdown inertial navigation error equations," *J. Guidance, Control and Dynamics*, vol. 25, no. 5, pp. 833–842, Sep. 2002.
[29] P. Savage, *Strapdown Analytics, Maple Plain*. Maple Plain, MN: Strapdown Associates, Inc., 2000, pp. 12-112–12-124.
[30] D. Goshen-Meskin and I. Y. Bar-Itzhack, "Unified approach to inertial navigation system error modeling," *J. Guidance, Control and Dynamics*, vol. 15, no. 3, pp. 648–653, May 1992.
[31] A. Papoulis, *Probability, Random Variables, and Stochastic Processes*, 3rd ed. New York: McGraw-Hill, 1991, p. 295.
[32] R. D. Yates and D. J. Goodman, *Probability and Stochastic Processes*. New York: Wiley, 1998, p. 328.
[33] K. Ogata, *Mordern Control Engineering*, 4th ed. Englewood Cliffs, NJ: Prentice-Hall, 2002, p. 286, 754.
[34] *C-MIGITS II Integrated GPS/INS User's Guide*. Anaheim, CA: Boeing North American Inc., 1997.

Songlai Han received the B.Sc. degree in electronic science and technology from Tianjin University, Tianjin, China, in 2003, and the M.Sc. degree in control science and technology from the National University of Defense Technology, Changsha, China, in 2005.

He is currently a joint-training doctorate candidate at both the National University of Defense Technology and the University of New South Wales, Sydney, Australia. His current research interests include INS, GPS/INS integration, multisensor fusion, and stochastic theory and its applications in navigation systems.

Jinling Wang received the B.Sc. degree in surveying/GNSS and the M.Sc. degree in surveying/GNSS from the Wuhan Technical University of Surveying and Mapping, Wuhan, China, in 1983 and 1990, respectively, and the Ph.D. degree in GPS/Geodesy from the Curtin University of Technology, Perth, Australia, in 1999.

He is currently an Associate Professor in the School of Surveying and Spatial Information Systems, University of New South Wales, Sydney, Australia. He has published over 200 papers in journals and conference proceedings. His current research interests include Global Navigation Satellite Systems (e.g., GPS, GLONASS) and their integration, augmentation of GPS with pseudolites, integration of INS and GPS/GLONASS, and statistical theory and its applications in positioning and navigation systems.

Dr. Wang is a Fellow of the Royal Institute of Navigation, U.K., and a Fellow of the International Association of Geodesy (IAG). He is a member of the Editorial Board for the International Journal *GPS Solutions*, and was Chairman of the study group (2003–2007) on pseudolite applications in positioning and navigation within the IAG's Commission 4. He was the 2004 President of the International Association of Chinese Professionals in Global Positioning Systems (CPGPS), and the Founding Editor-in-Chief for the *Journal of Global Positioning Systems* (2002–2007).